Engineering the Independent Folding of the Subtilisin BPN′ Pro-Domain: Correlation of Pro-Domain Stability with the Rate of Subtilisin Folding[†]

Lan Wang, Biao Ruan, Sergei Ruvinov, and Philip N. Bryan*

Center for Advanced Research in Biotechnology, University of Maryland Biotechnology Institute, 9600 Gudelsky Drive, Rockville, Maryland 20850

Received November 5, 1997; Revised Manuscript Received December 23, 1997

ABSTRACT: The 77-amino acid pro-domain greatly accelerates the in vitro folding of subtilisin in a bimolecular reaction whose product is a tight complex between folded subtilisin and folded pro-domain. In this complex the pro-domain has a compact structure with a four-stranded antiparallel β-sheet and two three-turn α-helixes. When isolated from subtilisin, however, the pro-domain is 97% unfolded even under optimal folding conditions. The instability of the isolated pro-domain suggests that there may be a thermodynamic linkage between the stability of the pro-domain and its ability to facilitate subtilisin folding. On the basis of the X-ray crystal structure of the pro-domain subtilisin complex, we have designed stabilizing mutations in three areas of the pro-domain: α-helix 23−32 (E32Q), β-strands 35−51 (Q40L), and α-helix 53−61 (K57E). These amino acid positions were selected because they do not contact subtilisin in the complex and because they appear to be in regions of the structure which are not well packed in the wild type pro-domain. Since none of the mutations directly contact subtilisin, their effects on the folding of subtilisin are linked to whether or not they stabilize a conformation of the pro-domain which promotes subtilisin folding. By sequentially introducing the three stabilizing mutations, the equilibrium for folding the pro-domain was shifted from 97% unfolded to 65% folded. By measuring the ability of these mutants to fold subtilisin, we are able to establish a correlation between the stability of the pro-domain and its ability to accelerate subtilisin folding. As the pro-domain is stabilized, the folding reaction becomes faster and distinctly biphasic. A detailed mechanism was determined for the double mutant, Q40L−K57E, which is 50% folded: $P + S_u \Leftrightarrow (30\ 800\ M^{-1}\ s^{-1}, 0.04\ s^{-1})\ PS_I \Leftrightarrow (0.07\ s^{-1}, <0.005\ s^{-1})\ PS$. PS_I is an intermediate complex which accumulates in the course of the reaction, and PS is the fully folded complex. The more stable the pro-domain, the faster the folding reaction up to the point at which the isomerization of the intermediate into the fully folded complex becomes the rate-limiting step in the folding process.

Subtilisin BPN′ is a 275-amino acid, serine protease secreted from the soil bacterium *Bacillus amyloliquefaciens*. Secretion and folding of subtilisin requires two separate processing steps on the initial precursor protein (*1*,*2*). The 30-amino acid signal peptide is removed during secretion. The extracellular part of the maturation process appears to involve folding of prosubtilisin, self-processing of the 77-amino acid pro-domain to produce a processed complex, and finally degradation of the pro-domain to create the 275-amino acid mature form of the enzyme (*3*,*4*). The reaction is similar to the folding of α-lytic protease, which is catalyzed by a 166-amino acid pro-domain (*5*−*7*). Both subtilisin and α-lytic protease are extracellular, bacterial, serine proteases, though they are not evolutionarily related.

In vitro mature subtilisin, when denatured and returned to native conditions, folds very slowly (*8*). Presumably, proteins must encode two pieces of information in order to fold. First the amino acid sequence must encode a native conformation which is a local energetic minimum, and second the protein must know how to solve the search problem and find the minimum (*9*). We have shown previously that the inactive subtilisin mutant Sbt70[1] is thermodynamically stable and therefore believe that its slow folding results from a lack of an efficient folding pathway (*10*). The isolated pro-domain has been shown in vitro to promote the folding of subtilisin in a bimolecular process whose product is a tight complex between the folded subtilisin and the folded pro-domain (*11*−*13*). The interaction of the pro-domain with subtilisin is believed to expedite the folding process by providing an energetically more favorable folding pathway.

In complex with subtilisin the pro-domain assumes a compact structure with a four-stranded antiparallel β-sheet and two three-turn α-helixes (*10*,*14*) (Figure 1). The folded pro-domain has shape complementarity and high affinity for native subtilisin (*15*). When isolated, however, the pro-

[†] This work was supported by NIH Grant GM42560.

* Corresponding author.

[1] Abbreviations: P, pro-domain; PS_I, the intermediate complex of pro-domain and partially folded subtilisin; PS, the complex of pro-domain and folded subtilisin; Pi, phosphate; pro-wt, wild type pro-domain of subtilisin BPN′; S, subtilisin; S_u, unfolded subtilisin; Sbt70, subtilisin BPN′ with the following mutations: K43N, M50F, A73L, Δ75-83, Q206V, Y217K, N218S, and S221A; Tris, tris(hydroxymethyl)aminomethane.

S0006-2960(97)02741-4 CCC: $15.00 © 1998 American Chemical Society
Published on Web 02/12/1998

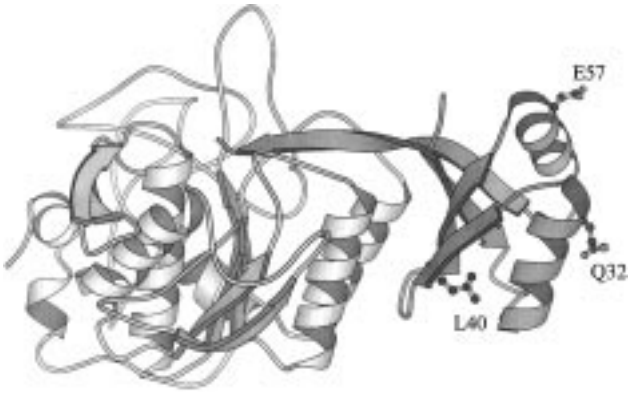

FIGURE 1: Structure of the E32Q−Q40L−K57E pro-domain in complex with Sbt70. Drawing depicting the α-carbon backbone of the bimolecular complex of subtilisin Sbt70 (lighter shading) and E32Q−Q40L−K57E (darker shading). The structure was determined by X-ray diffraction at 1.8-Å resolution (Almog et al., manuscript in preparation). The mutant side chains E32Q, Q40L, and K57E are shown in ball-and-stick representation. Notice that none of the mutant side chains contact subtilisin. Drawn with MOLSCRIPT (*24*).

domain is 97% unfolded even under optimal folding conditions (0.1 M KPi, pH 7.0, 20 °C), suggesting that there could be a thermodynamic linkage between the stability of the pro-domain and its ability to facilitate subtilisin folding. The wild type pro-domain is able to fold subtilisin Sbt70 at a rate of ∼500 M^{-1} s^{-1}. This rate is quite modest considering that collisions between subtilisin and the pro-domain occur at the rate of diffusion (e.g. ≥10^8 M^{-1} s^{-1}). To determine the linkage between the stability of the pro-domain and its ability to facilitate subtilisin folding, we have designed three mutations which stabilize the independent folding of the pro-domain. By sequentially introducing the three stabilizing mutations, the equilibrium for folding the pro-domain can be shifted progressively from 97% unfolded to 65% folded. This paper demonstrates that the rate of subtilisin folding can be greatly accelerated by stabilization of the pro-domain.

MATERIALS AND METHODS

Cloning and Expression of the Pro-Domain and Sbt70. Cloning and expression of Sbt70, wild type pro-domain, and mutants are as described (*10*,*15*).

Kinetics of Pro-Domain Binding to Native Sbt70. The rate of binding of pro-wt, K57E, Q40L, Q40L−K57E, and E32Q−Q40L−K57E to folded Sbt70 was monitored by fluorescence using a KinTek Stopped-Flow Model SF2001. The reaction was followed by the 1.2-fold increase in the tryptophan fluorescence of Sbt70 upon its binding of the pro-domain (*13*). Prodomain solutions of 10−160 μM in a 30 mM Tris-HCl, 5 mM KPi, pH 7.5 solution were mixed with an equal volume of a 2 μM subtilisin, 30 mM Tris-HCl, 5 mM KPi, pH 7.5 solution in a single mixing step. Typically 10−15 kinetics traces were collected for each [P]. The final [Sbt70] was 1 μM, and the final [P] values were 5−80 μM.

Kinetic Analysis of Pro-Domain-Facilitated Sbt70 Folding. Single Mixing. Refolding of subtilisin was followed by monitoring changes in tryptophan fluorescence (excitation, $\lambda = 300$ nm; emission, 340-nm cutoff filter) using a KinTek Stopped-Flow Model SF2001 for rapid kinetic measurements, as described (*10*). The reaction was followed by the 1.5-fold increase in the tryptophan fluorescence of Sbt70 upon folding of Sbt70 into its complex with the pro-domain. A stock solution of Sbt70 at a concentration of 100 μM in a 100 mM KPi, pH 7.0 solution was prepared for refolding studies. Sbt70 was denatured by diluting 20 μL of the Sbt70 stock solution into 1 mL of HCl solution (the final HCl concentration was 0.05 M). Sbt70 is completely denatured in less than 1 s by these conditions (*10*). The sample was neutralized by mixing the Sbt70 and HCl solution into an equal volume of 60 mM Tris-base, KPi, and pro-domain in the KinTek Stopped-Flow apparatus (final buffer concentrations were 30 mM Tris-HCl, 5 mM KPi, pH 7.5). The final concentration of Sbt70 was 1 uM, while the pro-domain concentration was varied from 5 to 20 μM. Typically 10−15 kinetics traces were collected for each [P].

Double Mixing. The kinetics of the formation of the folded complex PS were determined by a double-jump renaturation−denaturation experiment. The KinTek Stopped-Flow apparatus in the three-syringe configuration was used to perform the two mixing steps. In the first mixing step, 2 μM Sbt70 in 50 mM HCl is mixed with a variable concentration of pro-domain in 60 mM Tris-base and KPi. The resulting solution is 30 mM Tris-HCl, 5 mM KPi, pH 7.5. The final concentration of Sbt70 was 1 uM, while the pro-domain concentration was varied from 5 to 20 μM after the first mixing step. Sbt70 and pro-domain are allowed to fold under native conditions in the delay line of the stopped-flow apparatus for aging times ranging from 0.5 to 60 s. After the prescribed aging time the Sbt70−prodomain solution is mixed 2:1 with 0.1 M H_3PO_4 to bring the pH to 2.3. The stopped-flow apparatus collected fluorescence data for the denaturation of the folded complex after the second mixing step. The folded Sbt-70−prodomain complex denatures at a rate of 3.5 s^{-1} under these conditions. The amount of folded complex which accumulates during the aging time is calculated from the amplitude of the denaturation reaction. Typically 10−15 kinetic traces were collected for each [P].

RESULTS

Generation of Stable Folds. On the basis of the X-ray crystal structure of the pro-domain subtilisin complex (*10*,*14*), we have designed mutations which increase the independent stability of the pro-domain. Stabilizing mutations were identified in three different areas of the structure of the prodomain: α-helix 23−32 (E32Q),[2] β-strands 35−51 (Q40L), and α-helix 53−61 (K57E). These amino acid positions were selected because they do not contact subtilisin in the complex and because they appear to be in regions of the structure which are not well packed in the wild type pro-domain (Figure 1). The mutations in the two α-helixes were introduced to improve upon what appeared to be unfavorable electrostatic interactions in the folded state. In the first α-helix an ε-oxygen of E32 is separated by only 4 Å from a δ-oxygen of D28. The E32Q mutation was introduced to reduce electrostatic repulsion. In the second helix, three surface lysines (K54, K57, and K61) are located on consecutive α-helical turns, and thus the charged ε-amino groups are separated from one another by only 6−7 Å. To reduce

[2] A shorthand for denoting amino acid substitutions employs the single-letter amino acid code as follows: E32Q denotes the change of glutamate 32 to glutamine.

Table 1: Effects of Pro-Domain Mutations on Stability and Sbt70 Folding

	fraction of folded monomer[a]	k_1[b] (M^{-1} s^{-1})
57K	0.13	5 600
40L	0.15	8 400
40L−57E	0.50	30 800
E32Q−40L−57E	0.65	42 000

[a] The fractions of folded monomer were calculated as described in ref 16. [b] The rate constant for the binding step, k_1, is determined from the slope of the observed rates of the fast phase of the Sbt70-folding reaction versus $[P_{monomer}]$.

electrostatic repulsion, the K57E mutation was introduced. The Q40L mutation was introduced to improve the hydrophobic packing between β-strand 35−51 and α-helix 23−32 (*16*). Since none of the mutations directly contact subtilisin, their effects on the folding of subtilisin are linked to whether they stabilize a conformation of the prodomain which promotes subtilisin folding. The correct topology of the binding interface depends on the correct tertiary structure of the pro-domain with the four-stranded β-sheet correctly formed.

In addition to the single mutants, two double mutants and a triple mutant were also constructed. The double mutant is denoted 40L−57E. The triple mutant is denoted E32Q−Q40L−K57E. The stabilities of the pro-domain mutants have been determined previously (*16*) and are summarized in Table 1. The stabilities of the pro-domain mutants range from $\Delta G_{unfolding} = -2.1$ kcal/mol for pro-wt to $\Delta G_{unfolding} =$ 0.4 kcal/mol for E32Q−Q40L−K57E. The structure of E32Q−Q40L−K57E in complex with subtilisin was determined by X-ray crystallography (Almog et al., manuscript in preparation). No changes in α-carbon backbone are observed to result from the mutations on comparison of E32Q−Q40L−K57E to pro-wt.

Subtilisin Engineered for Facile Folding. Mature subtilisin BPN′, once denatured, refolds to the native state very slowly ($\tau >$ weeks) in the absence of the pro-domain (*8*). Even when catalyzed by the isolated pro-domain in a bimolecular reaction, refolding of subtilisin occurs at a rate of only ∼0.2 s^{-1} M^{-1} of pro-domain (*17*). The slow time scale of in vitro folding makes detailed kinetic analysis of the process problematic. To make the study of subtilisin folding more tractable, we have engineered a subtilisin for facile folding. A major part of the kinetic barrier to folding subtilisin involves formation of a high-affinity calcium binding site ($K_a = 10^7$ M^{-1} at 25 °C), called site A (*8*). Deletion of amino acids 75−83 removes the calcium A-site and destabilizes subtilisin but greatly accelerates both uncatalyzed folding and pro-domain-catalyzed folding (*8,13*). The subtilisin mutant used in these studies is denoted Sbt70 and contains the following mutations: Δ75−83 (to eliminate calcium binding and accelerate the folding rate); S221A (to remove the active site nucleophile and eliminate proteolytic activity); and six other substitutions which restore stability lost due to the calcium loop deletion (*18*). None of the mutant amino acids except A221 contact the pro-domain in the bimolecular complex. The folding reaction of Sbt70 with pro-wt has been described in (ref 10).

Analysis of Prodomain Binding to Native Subtilisin. Since the stabilizing mutations are introduced in regions of the pro-domain which do not directly contact subtilisin upon formation of the complex, their effects on binding to native subtilisin are linked to whether or not they stabilize the native conformation of the pro-domain. As the fraction of folded pro-domain approaches 1, the observed association constant approaches its maximum. We have previously shown that the 15−20-fold difference in the fraction of folded protein between Q40L−K57E and pro-wt results in a ≥15-fold difference in binding constant (*16*).

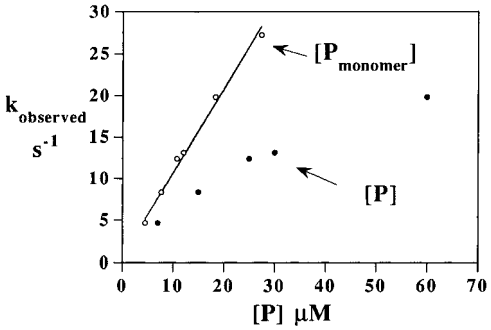

FIGURE 2: Binding rate of the pro-domain Q40L−K57E in the presence of folded Sbt70. Binding was monitored by fluorescence in 30 mM Tris-HCl, 5 mM KPi, pH 7.5 at 25 °C. The pseudo-first-order rate constant for binding, k_{obs}, is plotted with open circles versus $[P_{monomer}]$ and solid circles versus $[P_{total}]$. The k_{obs} was a linear function of $[P_{monomer}]$ and could be fit to the equation $k_{obs} = 0.5 + (1 \times 10^6 [P_{monomer}]$.

$$P + S \underset{k_{off}}{\overset{k_{on}}{\Leftrightarrow}} PS$$

To determine the rate constant for binding, k_{on}, the basic experiment is to measure the rate of the fluorescence changes which occur upon binding of the pro-domain to folded Sbt70. Fluorescence at 345 nm increases by 1.2-fold upon the binding of pro-domain to Sbt70. If the reaction is carried out with an excess of P, then one observes a pseudo-first-order kinetic process with $k_{obs} = k_{off} + k_{on}[P]$.

The rate of binding for Q40L−K57E is presented in Figure 2. The curvature in the plot of [P] versus k_{obs} is due to the tendency of Q40L−K57E to dimerize. The monomer−dimer equilibrium for this family of promutants has been studied previously by sedimentation equilibrium (*16*). We have measured the dimerization constant for each pro-domain mutant and have shown that there is a rapid equilibrium between monomer and dimer species. Under the conditions of the binding experiment, the dissociation constant for the dimerization of E32Q−Q40L−K57E is 10 μM and the dissociation constant for Q40L−K57E is 15 μM. The less stable pro-mutants have no detectable tendency to dimerize. By using a sufficient excess of pro-domain over Sbt70, the monomer concentration remains almost constant over the course of the binding reaction. This can be seen from the linearity of a plot of k_{obs} versus $[Q40L-K57E_{monomer}]$ (Figure 2). The slope of the plot yields $k_{on} = 1.0 \times 10^6$ M^{-1} s^{-1} for the binding of monomer to folded Sbt70. In fact all prodomain mutants have similar rates for the binding of $P_{monomer}$ to Sbt70. The rate constants range from 8×10^5 M^{-1} s^{-1} for pro-wt to 1.0×10^6 M^{-1} s^{-1} for $Q40L-K57E_{monomer}$. This kinetic behavior for binding suggests that only pro-domain monomers bind to Sbt70. Other evidence for the binding of the monomer species comes from the one to one stoichiometry of binding determined from titration calorimetric experiements (*16*) and from the X-ray structures

of one to one complexes determined for pro-wt (*10*) and E32Q−Q40L−K57E (Almog et al., manuscript in preparation) with Sbt70.

Transient State Kinetic Analysis of Prodomain-Facilitated Sbt70 Folding. The proposed mechanism of pro-domain-catalyzed Sbt70 folding is as follows:

$$P_u \overset{K_{eq}}{\Longleftrightarrow} P + S_u \underset{k_{-1}}{\overset{k_1}{\Longleftrightarrow}} PS_I \underset{k_{-2}}{\overset{k_2}{\Longleftrightarrow}} PS$$

where P_u is unfolded pro-domain, P is folded pro-domain, S_u is unfolded subtilisin, S is folded subtilisin, PS_I is a collision complex of a partially folded subtilisin intermediate and folded pro-domain, and PS is the complex of folded subtilisin and folded pro-domain (*13*). We have employed transient state kinetic measurements to identify kinetic intermediates and determine the microscopic rate constants for the reaction (*19*).

Single Mixing. The basic kinetic experiment is to mix unfolded Sbt70 with an excess of pro-domain in the stopped flow fluorimeter and to measure the rates and amplitudes of fluorescence changes during a single turnover of subtilisin folding. The folding reaction of subtilisin, in the presence of pro-domain, can be followed by an increase in tryptophan fluorescence due to changes in the environments of the three tryptophans in subtilisin upon its folding and binding of the pro-domain. The pro-domain does not contain tryptophan residues and thus has no intrinsic fluorescence above 345 nm upon excitation at 300 nm. Therefore fluorescence increases observed at 345 nm are due solely to the conversion of S_u to PS_I and PS.

If denatured and returned to native conditions at low ionic strength, Sbt70 is kinetically isolated from the native state. At 30 mM Tris, 5 mM KPi, pH 7.5, the rate of uncatalyzed folding of Sbt70 is $<5 \times 10^{-5}$ s^{-1} at 25 °C. When the isolated pro-domain is added, the rate of subtilisin folding increases rapidly with the concentration of pro-domain monomer, $[P_{monomer}]$. The folding reaction was followed using $[S_u] = 1$ μM and $[P_{monomer}] = 5$ μM for each of the mutant pro-domains. The product is a one to one complex of Sbt70 and pro-domain. All of the single pro-domain mutations increased the rate of subtilisin folding (Figure 3). The folding curves of pro-wt and the E32Q promutant can be fit with a single-exponential equation. As the stability of the pro-domain increases, however, the folding reactions deviate from single-exponential kinetics. The folding reactions of Sbt70 with the mutants Q40L, K57E, 40L−57E, and E32Q−Q40L−K57E are faster than those with pro-wt and distinctly biphasic (Figure 4). The biphasic kinetics suggest that an intermediate state becomes populated in the course of the folding reaction. Plotting the rate constants (k_1) for the fast phase of the folding reaction for Q40L, K57E, Q40L−K57E, and E32Q−Q40L−K57E versus the fraction of folded pro-domain (data in Table 1) yields a straight line ($R = 0.999$) with a slope of ~68 000 s^{-1} per mole of folded prodomain.

To learn more about the nature of the intermediate state, the rates and amplitudes of the two kinetic phases were analyzed in detail using Q40L−K57E. Plotting the rate of the fast phase of the reaction versus $[P_{monomer}]$ yields a straight line with a slope of 30 800 M^{-1} s^{-1} and an intercept of 0.11 s^{-1} (Figure 5A). The amplitude of the fast phase increases as $[P_{monomer}]$ increases (Figure 5B). At $[P_{monomer}] > 20$ μM the amplitude of the fast phase levels off at a value which is 85% of the total fluorescence change. The rate of the slow phase of the reaction increases hyperbolically with $[P_{monomer}]$ and reaches a value of ~0.07 s^{-1} at $[P_{monomer}] > 20$ μM. The amplitude of the slow phase decreases as $[P_{monomer}]$ increases. At $[P_{monomer}] > 20$ μM the amplitude of the slow phase levels off at a value which is 15% of the total fluorescence change.

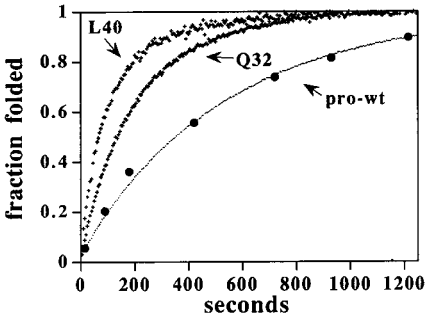

FIGURE 3: Effect of pro-domain mutations on the kinetics of subtilisin folding. 1 μM denatured Sbt70 and 5 μM pro-domain were mixed in 5 mM KPi, 30 mM Tris, pH 7.5 at 25 °C. The reaction was followed by the increase in tryptophan fluorescence which occurs upon folding of subtilisin into the pro-domain subtilisin complex. The data for pro-wt and 32Q can be fit to a single-exponential equation to determine a pseudo-first-order rate constant for folding of 0.0018 s^{-1} for pro-wt and 0.0043 s^{-1} for 32Q. Sbt70 folding with Q40L is the fastest of the three but is not a single-exponential phase. The solid circles show the rate of Sbt70 folding with pro-wt as measured by double-jump renaturation−denaturation, as described in the text.

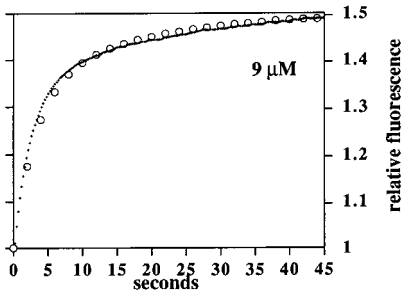

FIGURE 4: Folding rate of Sbt70 in the presence of Q40L−K57E. 9 μM Q40L−$K57E_{monomer}$ and 1 μM denatured Sbt70 were mixed in 5 mM KPO_4, 30 mM Tris, pH 7.5. The temperature was 25 °C. The reaction was followed by the increase in tryptophan fluorescence which occurs upon folding of subtilisin into the pro-domain subtilisin complex. The open circles are calculated using KINSIM using the mechanism described in the text.

On the basis of the analysis of Sbt70 folding as a function of [Q40L−$K57E_{monomer}$], we tentatively concluded that the fast phase of the fluorescence increase defines the formation of PS_I (the binding phase) and the slow phase defines the decay of PS_I and the formation of PS. The slope of the fast phase rate versus [Q40L−K57E] yields $k_1 = 30\,800$ M^{-1} s^{-1}. The *y*-intercept of the plot yields $k_{-1} + k_2 + k_{-2} = 0.11$ s^{-1} (Figure 5A). The slow phase of the reaction reaches a maximum rate of $k_2 + k_{-2} = 0.07$ s^{-1}. The value of k_{-2} cannot be accurately determined in these experiments but must be much smaller than k_2 since the overall equilibrium for the reaction lies far in the direction of PS.

To check the fitness of our kinetic model, the rates and amplitudes of the two phases over a range of [P] were simulated using KINSIM (*20*,*21*). The kinetic model used

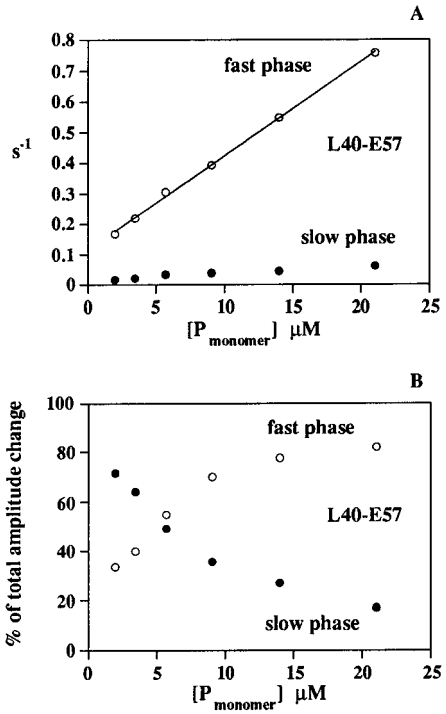

FIGURE 5: Plot of rates and amplitudes for folding of Sbt70 and Q40L−K57E. Time courses for folding as followed by fluorescence (as shown in Figure 4) were fit to double-exponential equations. The rate constants for the fast and slow phases plotted versus $[P_{monomer}]$ are shown in part A. The amplitudes for the fast and slow phases plotted versus $[P_{monomer}]$ are shown in part B.

to generate the fit is

$$P + S_u \underset{0.04\ s^{-1}}{\overset{30\ 800\ M^{-1}}{\leftrightarrow}} PS_I \underset{<0.005\ s^{-1}}{\overset{0.07\ s^{-1}}{\leftrightarrow}} PS$$

The fluorescence of PS is known to be 1.5-times that of S_u. The agreement between the simulation and the data is good if the fluorescence of PS_I is assigned to be 1.425-times the fluorescence of S_u. An experimental curve and the KINSIM fit are shown in Figure 4.

Double Mixing. The kinetic model which we have proposed makes specific predictions about the rate of accumulation of a fully folded complex. We therefore designed a double-mixing experiment to directly measure the rate of accumulation of the folded complex, PS, as a function of [P] during a single turnover of subtilisin folding. The first step mixes unfolded Sbt70 with an excess of pro-domain and allows the two to react for an aging time under native conditions (30 mM Tris-HCl, pH 7.5). In the second step the aged mixture is mixed with phosphoric acid, bringing the sample to pH 2.3. The rate of acid denaturation for the fully folded complex at pH 2.3 is 3.5 s^{-1}. This turns out to be much slower than the rate of denaturation of PS_I (>100 s^{-1}). Thus by measuring the fluorescence amplitude of the acid denaturation phase as a function of the aging time of the folding reaction, we are able to follow the accumulation of folded complex (*22*) (Figure 6).

Figure 3 shows the rate of accumulation of PS as a function of [pro-wt] measured by double mixing and single mixing. The double- and single-mixing experiments show the same single-exponential kinetics because the rate of formation of PS is a one-step reaction in the presence of excess pro-wt. Both experiments are thus measuring the

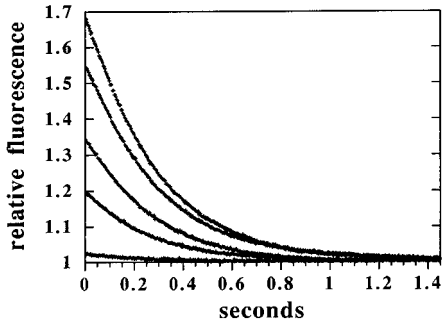

FIGURE 6: Double-jump renaturation−denaturation experiment. Denatured Sbt70 and Q40L−K57E were returned to the native condition (30 mM Tris, pH 7.5, 25 °C) and allowed to fold for aging times of 0.5, 5, 10, 20, and 30 s. In the second step the aged mixture is mixed with phosphoric acid, bringing the sample to pH 2.3. The rate of acid denaturation for the fully folded complex at pH 2.3 is 3.5 s^{-1}. The amplitude of the denaturation reaction is determined for each aging time to determine how much folded complex has accumulated.

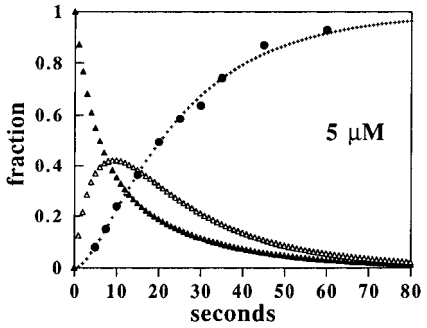

FIGURE 7: KINSIM simulated species analysis with experimentally determined kinetics of PS formation. KINSIM was used to calculate the fraction of S_u, PS_I, and PS as a function of folding time using the rate constants given in the text. The fraction of S_u is shown by solid triangles, the fraction of PS_I is shown by open triangles, and the fraction of PS is shown by the dashed line. Solid circles show the accumulation of PS experimentally determined by a double-jump renaturation−denaturation experiment using 5 μM Q40L−K57E$_{monomer}$ and 1 μM denatured Sbt70.

formation of PS because PS_I does not accumulate to high enough levels to be kinetically detectable.

The rate of accumulation of PS as a function of [Q40L−K57E] is shown in Figure 7. The formation of PS is a function of all four microscopic rate constants with the maximum rate equal to $k_2 + k_{-2}$. KINSIM was used to calculate the accumulation of PS_I and PS as a function of folding time using the rate constants given above. At four different [Q40L−K57E] values, the rate of accumulation of PS, as determined in double-mixing experiments, was found to match its calculated rate of formation. At the lower [Q40L−K57E] there is a lag in the production of PS, as the formation of PS_I is limiting early in the reaction. At the higher [Q40L−K57E] PS_I forms rapidly and the production of PS is almost a single-exponential process with very little lag.

Summary of Kinetic Results for Q40L−K57E. The kinetics of the fluorescence increase in a single-mixing renaturation experiment are biphasic, indicating a minimal two-step reaction mechanism. Plotting the rate of the fast fluorescence increase versus [Q40L−K57E] defines the rate of the binding phase of the reaction. The fast phase of the reaction is linear with [Q40L−K57E] and the slope defines k_1, the second-order rate constant for formation of PS_I (30 800 M^{-1} s^{-1}).

The *y*-intercept of the plot defines the decay of PS_I and is equal to $k_{-1} + k_2 + k_{-2}$ (0.11 s^{-1}). Folding from S_u into PS_I accounts for 85% of the total fluorescence increase. The slow phase of the fluorescence change corresponds to the decay of the initial complex (PS_I) and the formation of the fully folded complex (PS). Isomerization of PS_I into PS accounts for the remaining 15% of the total fluorescence increase. The maximum rate of the isomerization step is equal to $k_2 + k_{-2}$ (0.07 s^{-1}). (The rate of PS formation also was determined by double-mixing renaturation−denaturation experiments.) Since $k_{-1} + k_2 + k_{-2}$ was determined to be 0.11 s^{-1} then k_{-1} is 0.04 s^{-1}. The equilibrium constant for the formation of PS_I can be determined from $k_1/k_{-1} = 8 \times 10^5$ M^{-1}.

The constant k_{-2} is small (<0.005 s^{-1}) but not defined in these experiments. The ratio of k_2/k_{-2} defines the equilibrium between PS_I and PS. The X-ray structure of this complex shows subtilisin to have the native fold; thus, the equilibrium must lie toward the folded complex. Determining the exact ratio of k_2 and k_{-2} will be important for understanding the mechanism of catalysis, because these rates are determined by the energetic barrier between the intermediate and the folded complex. These experiments are in progress.

Q40L−K57E has thus been very useful in establishing a two-step folding mechanism because the intermediate, PS_I, accumulates to easily detectable levels at micromolar concentrations of Q40L−K57E. At micromolar concentrations of pro-wt and single mutants, PSI is not kinetically detectable; thus, formation of the fully folded complex appears as a single kinetic step.

DISCUSSION

Prosubtilisin has a facility for folding which the stable, mature enzyme lacks, suggesting that efficient folding pathways are not a necessary consequence of a stable native state. An efficient folding pathway implies that productive intermediates are significantly more stable than the surrounding landscape of unfolded and misfolded conformations. Native folding intermediates of mature subtilisin may have similar or lower stability than unfolded or misfolded states. This would result in a large entropic barrier to folding, since most of the native structure would have to be formed before a significant free energy well is reached in conformational space.

In pro-domain-assisted Sbt70 folding, the stability of an intermediate complex determines the overall folding rate. Analysis of the five pro-domain mutants described here shows a correlation between the stability of the pro-domain and its ability to accelerate folding. The first step is the association of the pro-domain with subtilisin to form the intermediate PS_I. With a stabilized pro-domain, such as Q40L−K57E, this interaction is fairly strong ($K_a = 8 \times 10^5$ M^{-1}). We can consider that PS_I is a folding intermediate which is stabilized by pro-domain mutations. The more stable the intermediate, the faster the folding reaction up to the point at which the isomerization of the intermediate into the fully folded complex becomes the rate-limiting step. For example, at 20 μM Q40L−K57E, virtually all unfolded subtilisin is rapidly bound in the intermediate complex and the folding reaction approaches its maximum rate.

The structure of the pro-domain subtilisin complex suggests that the pro-domain promotes folding by stabilizing the 100−144 $\alpha\beta\alpha$ motif in subtilisin (*10*,*14*). The folded pro-domain is a compact structure with shape complementarity and high affinity for native subtilisin. The pro-domain binds on subtilisin's two parallel surface α-helixes and supplies caps to the N-termini of the two helixes and may selectively stabilize the $\alpha\beta\alpha$ motif relative to other partially folded states (Figure 1). We propose that the pro-domain bound to the $\alpha\beta\alpha$ substructure corresponds to the collision complex, PS_I. Both the pro-domain and the 45-amino acid $\alpha\beta\alpha$ motif are proposed to have a more or less native fold in the bimolecular intermediate (*15*).

Even though stabilization of the $\alpha\beta\alpha$ motif appears to be the mechanism by which the pro-domain catalyzes folding of Sbt70, folding may also be accelerated by stabilizing other intermediate structures. We have previously shown that early organization of the structure around amino acids 22 and 87 resulting from a disulfide cross-link accelerates uncatalyzed subtilisin folding by 850-fold (*23*). The slow step in the Sbt70 folding reaction may be forming any initial structure capable of propagating folding. A mutation (or pro-domain binding) which stabilizes a partially folded topology may therefore accelerate the folding rate. Subtilisin inhibitors which bind tightly as substrates in the active site do not accelerate folding, however. Presumably this is because formation of the active site involves substantial tertiary structure and hence is after the rate-limiting step in the folding process.

If the independent stability of the pro-domain determines the overall subtilisin folding rate, why would nature not select for a more stable pro-domain? This may be because of the thermodynamic linkage between stabilizing pro-domain mutations and binding affinity for native subtilisin. As the fraction of folded pro-domain approaches 1, the observed association constant with subtilisin approaches its maximum. This phenomenon is illustrated with 40L-57E. The 15−20-fold difference in the fraction of folded protein between 40L−57E and pro-wt results in a >15-fold increase in binding constant. The final step in subtilisin biosynthesis is the release of the pro-domain to generate active subtilisin. With an independently folded pro-domain, this final step may become rate limiting. Thus the pro-domain may have evolved a stability which is adequate for getting subtilisin folded but not so stable that it is a long-lived inhibitor of subtilisin.

ACKNOWLEDGMENT

The authors wish to thank Richard Prescott for synthesizing the oligonucleotides used in site-directed mutagenesis and DNA sequencing and Patrick Alexander and Susan Strausberg for useful discussion.

REFERENCES

1. Wells, J. A., Ferrari, E., Henner, D. J., Estell, D. A., and Chen, E. Y. (1983) *Nucleic Acids Res. 11*, 7911−7925.
2. Vasantha, N., Thompson, L. D., Rhodes, C., Banner, C., Nagle, J., and Filpula, D. (1984) *J. Bacteriol. 159*, 811−819.
3. Power, S. D., Adams, R. M., and Wells, J. A. (1986) *Proc. Natl. Acad. Sci. U.S.A.* 83, 3096−3100.
4. Ikemura, H., Takagi, H., and Inouye, M. (1987) *J. Biol. Chem. 262*, 7859-7864.
5. Baker, D., Silen, J., and Agard, D. (1992) *Proteins: Struct., Funct., Genet. 12*, 339−344.

6. Baker, D., Sohl, J., and Agard, D. A. (1992) *Nature 356*, 263−265.
7. Baker, D., and Agard, D. (1994) *Biochemistry 33*, 7505−7509.
8. Bryan, P., Alexander, P., Strausberg, S., Schwarz, F., Wang, L., Gilliland, G., and Gallagher, D. T. (1992) *Biochemistry 31*, 4937−4945.
9. Levinthal, C. (1968) *J. Chim. Phys. 65*, 44−45.
10. Bryan, P., Wang, L., Hoskins, J., Ruvinov, S., Strausberg, S., Alexander, P., Almog, O., Gilliland, G., and Gallagher, T. D. (1995) *Biochemistry 34*, 10310−10318.
11. Zhu, X., Ohta, Y., Jordan, F., and Inouye, M. (1989) *Nature 339*, 483−484.
12. Eder, J., Rheinnecker, M., and Fersht, A. R. (1993) *Biochemistry 32*, 18−26.
13. Strausberg, S., Alexander, P., Wang, L., Schwarz, F., and Bryan, P. (1993) *Biochemistry 32*, 8112−8119.
14. Gallagher, T. D., Gilliland, G., Wang, L., and Bryan, P. (1995) *Structure 3*, 907−914.
15. Wang, L., Ruvinov, S., Strausberg, S., Gallagher, T. D., Gilliland, G., and Bryan, P. (1995) *Biochemistry 34*, 15415−15420.
16. Ruvinov, S., Wang, L., Ruan, B., Almog, O., Gilliland, G., Eisenstein, E., and Bryan, P. (1997) *Biochemistry 36*, 10414−10421.
17. Eder, J., Rheinnecker, M., and Fersht, A. R. (1993) *J. Mol. Biol. 233*, 293−304.
18. Strausberg, S., Alexander, P., Gallagher, D. T., Gilliland, G., Barnett, B. L., and Bryan, P. (1995) *Biotechnology 13*, 669−673.
19. Johnson, K. A. (1992) *The Enzymes 20*, 1−61.
20. Barshop, B. A., Wrenn, R. F., and Frieden, C. (1983) *Anal. Biochem. 130*, 134−145.
21. Zimmerle, C. T., Patane, K., and Frieden, C. (1987) *Biochemistry 26*, 6545−6552.
22. Kiefhaber, T., Quaas, R., Hahn, U., and Schmid, F. X. (1990) *Biochemistry 29*, 3053−3061.
23. Strausberg, S., Alexander, P., Wang, L., Gallagher, D. T., Gilliland, G., and Bryan, P. (1993) *Biochemistry 32*, 10371−10377.
24. Kraulis, P. J. (1991) *J. Appl. Crystallogr. 24*, 946−950.

BI972741R